

# Lawrence Berkeley National Laboratory

## LBL Publications

### Title

Compressive Creep of Polymer Electrolyte Membranes: A Case Study for Electrolyzers

### Permalink

<https://escholarship.org/uc/item/4164c0xh>

### Journal

ACS Applied Energy Materials, 4(4)

### ISSN

2574-0962

### Authors

Arthurs, Claire  
Kusoglu, Ahmet

### Publication Date

2021-04-26

### DOI

10.1021/acsaem.0c03024

Peer reviewed

# Compressive Creep of Polymer Electrolyte Membranes: A Case Study for Electrolyzers

Claire Arthurs<sup>†,‡</sup> and Ahmet Kusoglu<sup>\*,†</sup>

<sup>†</sup>*Energy Conversion Group, Lawrence Berkeley National Laboratory, Berkeley, CA, 94720.*

<sup>‡</sup>*Department of Mechanical Engineering, University of California Berkeley, Berkeley, CA, 94720.*

E-mail: akusoglu@lbl.gov

## Abstract

For proton-exchange membrane (PEM) water electrolyzers to be commercially feasible, PEMs must perform over long lifetimes in liquid environments under compression while maintaining mechanical stability. Hydrated environment, while inherent for operation and conductivity, undermines PEM stability. Mechanical stability of PEMs is commonly characterized in tension, which is not applicable to electrolyzers, wherein PEMs could undergo high pressures. In this study, a compression creep procedure is developed using a custom-designed setup to monitor creep response of hydrated PEMs. Our results show PEMs exhibit continuous creep response under compression over 24 hours, with a dependence on the applied pressure and hydration state.

**Keywords:** compression, electrolyzer, creep, ionomer, mechanics, hydration

Proton-exchange membrane (PEM) water electrolyzers (PEMWEs) are a promising clean energy technology for electrochemical generation of hydrogen by splitting water. PEMWEs use an ion-conductive polymer, or ionomer, membrane to conduct protons from the anode to cathode while inhibiting crossover of electrons and product gases (O<sub>2</sub>, H<sub>2</sub>). PEMWEs

17 offer a variety of end-uses in industry and power generation because hydrogen is essential to  
18 many industrial applications, such as turbine blanketing gas, semiconductors, heat treating,  
19 and submarines for O<sub>2</sub>, and industrial gas applications. Hydrogen's energy capacity can be  
20 directly used in PEM fuel cells (PEMFCs).

21 Electrolyzers provide decarbonized hydrogen unlike methane reforming, currently the  
22 most common method of industrial hydrogen gas production.<sup>1</sup> For electrolyzers to compete  
23 with methane reforming, capital cost of these devices must be reduced.<sup>1,2</sup> To achieve cost  
24 reduction, thinner, more durable membranes are needed.<sup>2-5</sup> Improved durability of thinner  
25 PEMs is important for cost reduction of PEM electrolyzers<sup>3,4,6</sup> because PEMs must perform  
26 over 80,000 hours in electrolyzers in liquid environments according to the Department of  
27 Energy's hydrogen program goals.<sup>7</sup> Currently, most PEMWEs are operated at 1.5 - 3.0 MPa  
28 (15 - 30 bar) differential pressure and 30 - 50 °C.<sup>3</sup> However, higher pressure (> 35 MPa or  
29 350 bar) and high temperature (>50 °C) operation is desirable for PEM electrolysis.<sup>2,4,5,8</sup>  
30 Higher pressure allows electrolyzers to deliver hydrogen at a high pressure to the end user  
31 thus reducing the additional compressor cost and energy needed to compress and store the  
32 gas.<sup>2,4,8</sup> High pressure operation also allows for design flexibility for optimizing product gas  
33 removal.<sup>2,4,9</sup> However, operating at high differential pressure across the active area increases  
34 the required sealing pressures to prevent off-board leaks, thus further increasing the internal  
35 compressive stresses experienced by the active area of the electrolyte.<sup>8</sup> High pressure acting  
36 on the active area in PEMWE makes compressive creep a great concern which could im-  
37 pact the interfacial resistance between the membrane and the electrodes.<sup>2,10</sup> From a PEM  
38 perspective, high pressure deteriorates efficiency by increasing gas crossover (product loss)  
39 and induces larger stresses in the membrane which may compromise their mechanical sta-  
40 bility.<sup>2,4,5,9</sup> For this reason, industry has favored thicker membranes in PEMWEs, however,  
41 this increases the capital and operating cost since the electrical expense increases due to  
42 higher voltages resulting from the increase in ohmic resistance. Therefore, to overcome the  
43 challenges of improving PEMWE performance and durability, one must develop an accurate

44 way of assessing PEM mechanical stability by accounting for the effect of compression.

45 The prototypical PEM in acid-based low-temperature electrolyzers is perfluorosulfonic  
46 acid (PFSA) due to its mechanical and chemical stability and high ionic conductivity.<sup>11</sup>  
47 Most previous studies on the mechanical stability of PFSA investigated its mechanical  
48 properties only in tension.<sup>11</sup> However, in electrochemical devices, membranes undergo com-  
49 pression loads arising from a combination of assembly loads (pressures) and hydration-driven  
50 expansion within the constraints of the device geometry and edge effects, as discussed to a  
51 large extent in the fuel-cell literature.<sup>12,13</sup> Compression behavior, however, is even more crit-  
52 ical for understanding membrane behavior and durability in electrolyzers, where the PEM  
53 experiences a high-pressure, hot liquid environment during longer operating times. Fur-  
54 thermore, creep failure has been observed in Nafion-type membranes, especially at elevated  
55 temperature such as 80 °C.<sup>2,10</sup> Thus, for electrolyzers, it is even more imperative that creep  
56 be studied in a compressive mode, especially in water, as this is more relevant to device  
57 operation and will inform device lifetime.

58 The tensile stress-strain response of PFSA membranes is widely-studied and known to  
59 be highly sensitive to the surrounding environment, particularly, temperature and hydra-  
60 tion.<sup>11,14-19</sup> However, as shown in Figure 1b, the monotonic stress-strain response of PFSA  
61 is very different between tension and compression. In tension, the membrane exhibits a  
62 stress-strain response typical of semi-crystalline polymers; a linear elastic region followed by  
63 strain hardening after the onset of yielding, ending with failure. In compression, a mono-  
64 tonic, nonlinear increase in stress is observed. For a given strain, the membrane experiences  
65 much higher stress under compression than in tension. These findings indicate that creep  
66 behavior will also be disparate between the two stress-states.

67 It should be noted that this comparison between tension and compression is performed  
68 on Nafion 212, a dispersion-cast membrane, which is more commonly used in fuel-cell stud-  
69 ies, whereas electrolyzer studies predominantly use the thicker Nafion membranes (N11x  
70 series, where x=5, 7, 10).<sup>2,3,11</sup> Extruded membranes exhibit anisotropy in their mechani-

71 cal properties, primarily between the extruded “machine” direction and the transverse di-  
72 rection.<sup>11,14,18,20,21</sup> This anisotropy in mechanical properties could be linked to the intrin-  
73 sic structural anisotropy in membranes observed via x-ray scattering studies.<sup>12,13,21</sup> Cast  
74 membranes, on the other hand, have been shown to be less anisotropic in the plane, both  
75 structurally and mechanically.<sup>12,21,22</sup> Moreover, morphological domain-alignment occurring  
76 in Nafion membranes, whether induced intrinsically through manufacturing (cast vs. ex-  
77 truded) or externally through (pre/post)stretching, is related to anisotropy observed for  
78 transport properties, such as diffusion and conductivity.<sup>11–13,22–24</sup> However, it was also shown  
79 that, any intrinsic morphological anisotropy in Nafion membranes, especially in an extruded  
80 one, can be reduced upon boiling in water, which serves as part of a pretreatment procedure  
81 commonly employed in Nafion membrane studies.<sup>11,12,21</sup> Therefore, a dispersion-cast Nafion  
82 is selected to clearly demonstrate the disparity between tension and compression, but in the  
83 following, for the purposes of investigating the compression creep relevant to electrolyzer  
84 conditions, extruded Nafion 11x series will be employed in pretreated form (see supporting  
85 information (SI) for details on sample preparation).

86 In this study, we have developed a novel technique to study the creep compression of  
87 PEMs *in-situ* with controlled temperature and hydration, from ambient (referred to as dry,  
88 40-55% RH, 25-30 °C) to hydrated fully with liquid water (referred to as wet). The set-up,  
89 inspired from a design by Budinski et al.<sup>25</sup> and prior works of Kusoglu et al.,<sup>12,13,26</sup> is shown  
90 in Figure 1a and the experimental procedure explained in the SI.

91 Creep occurs when a material held under a constant stress over time generates a strain re-  
92 sponse. For a perfectly elastic material with no time-dependent response, no creep would oc-  
93 cur. Creep deformation in polymers is governed by the time-dependent changes in their mor-  
94 phology due to segmental mobility of polymer chains or relaxation of the network in response  
95 to constant load. In ionomers, creep response is also dependent on the hydration-driven  
96 dynamic changes in the structure, as previously shown for PFSA under tension.<sup>11,15,27–29</sup>

---

\*During a wet compression test, the membrane is in a bath of liquid DI water whereas in wet tension, the membrane was fully hydrated just prior to the experiment

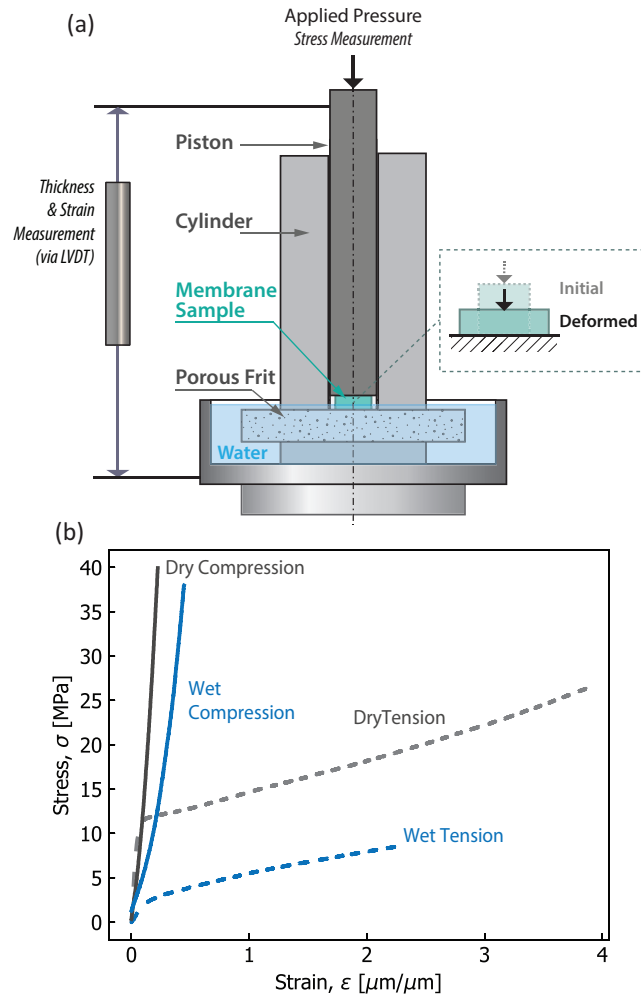


Figure 1: (a) Custom experimental compression setup with liquid water chamber. (b) Monotonic compression and tension of Nafion 212 in dry (ambient RH) and wet (fully hydrated) states. In tension, dry Nafion 212 exhibits a characteristic elastic-plastic response with an onset of non-linearity at 10 MPa, followed by strain hardening. In compression, however, the response is stiffer and nonlinear without a discernible yield point. Hydration of the membrane reduces its stiffness in both compression and tension mode while still preserving the characteristic response for each mode.\*

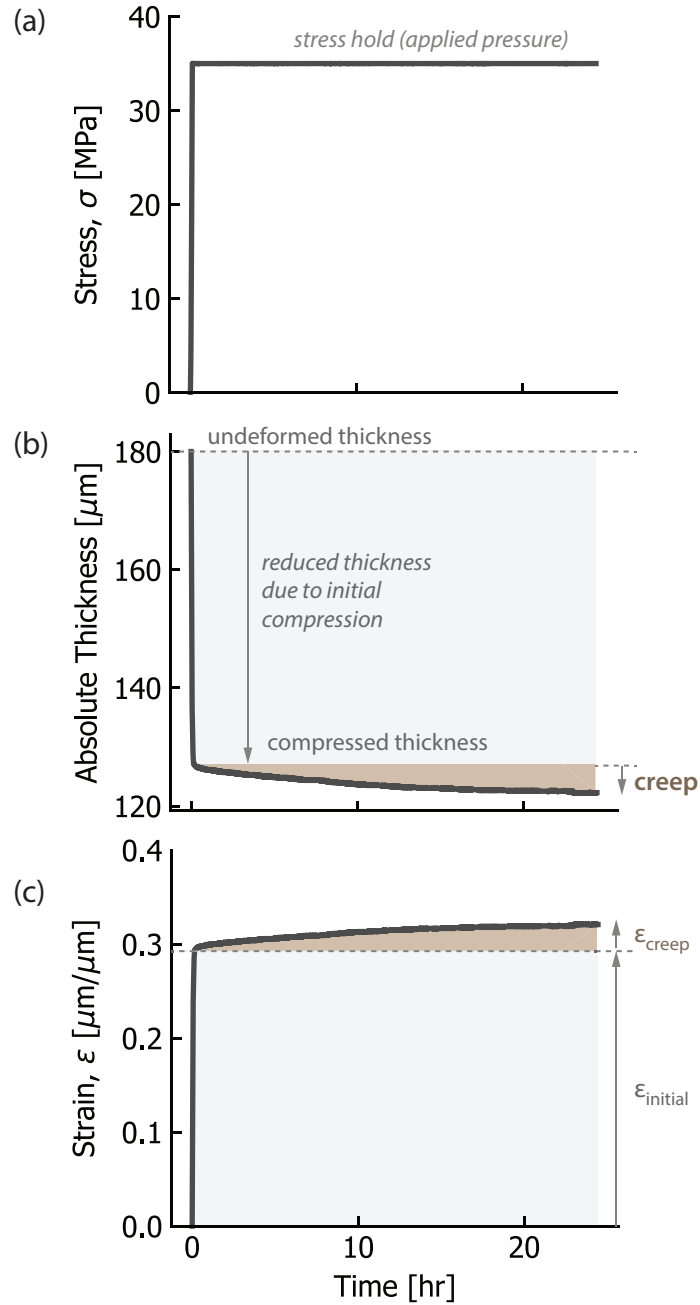


Figure 2: Compressive creep response of Nafion 117 PB for 24 hours at 35 MPa (350 bar). (a) The applied stress over time as the controlled input into the system. A quick ramp is applied followed by a constant load at 35 MPa (held for creep). (b) The measured output as the reduced membrane thickness over time due to compression (ramp) and then creep (hold). (c) The resulting compressive strain in the sample, which is defined positive. The ramp generates an initial strain, and then as the load is held, the thickness reduces over time corresponding to a positive increase in the strain, which is the creep strain.

97 While it has not been measured previously, creep is expected to occur in a compressed  
 98 PFSA as well.<sup>2,10</sup> PFSA ionomers have a phase-separated nanostructure resulting from the  
 99 molecular hydration of their ionic groups forming hydrophilic nano-domains separated by  
 100 the hydrophobic fluorocarbon backbone. While the hydrophilic domains impact PEM's ion  
 101 and water transport functionality across time and length-scales, the overall phase-separated  
 102 structure governs mechanical properties.<sup>11</sup> This dynamic, chemically-heterogeneous struc-  
 103 ture of PFSA also makes its mechanical behavior dependent on time, temperature, and  
 104 hydration.<sup>11,14–19,28,29</sup> Thus, to better mimic the environment an ionomer undergoes in an  
 105 electrolyzer, creep response of PFSA is monitored under compression, as shown in Figure 2.  
 106 Under a compression-type load, a compressive strain, or initial strain ( $\varepsilon_{initial}$ ), develops in  
 107 the membrane. When the applied stress is held constant, the membrane thickness decreases  
 108 further over time, indicating creep response. The change in strain over time represents the  
 109 creep strain ( $\varepsilon_{creep}$ ). The total strain can therefore be decomposed into the initial and the  
 110 creep strain as:

$$111 \qquad \qquad \qquad \varepsilon_{total} = \varepsilon_{initial} + \varepsilon_{creep}. \qquad (1)$$

112 Building upon the compelling evidence for compressive creep in PFSA, in the following,  
 113 we investigate the effect of hydration, applied pressure, and thickness.

114 Figure 3a shows compression creep of Nafion 117 at two pressure levels in dry and wet  
 115 states at 25 °C. It is relevant to note that strain is normalized with respect to initial thickness  
 116 of the membrane in the equilibrium condition (either wet or at ambient conditions). In  
 117 the wet state, there is a highly transient primary creep stage for the first hour, where  
 118 approximately 80% of the creep strain develops (Figure 3b). Then, a period of slower creep  
 119 ensues. Whereas, for the dry case, creep strain develops more linearly over time. Table  
 120 1 shows the creep strain and displacement rate over the whole length of the experiments.  
 121 By splitting the creep into two stages, 0-1 hr and 1-24 hr, additional comparison can be  
 122 made. In the secondary state, the dry membrane under 35 MPa exhibits the highest creep  
 123 strain rate,  $\dot{\varepsilon}_{creep} = 1.30 \times 10^{-3} \text{ hr}^{-1}$ , whereas the wet membrane at 35 MPa exhibits the



124 lowest creep strain rate,  $\dot{\epsilon}_{creep} = 0.484 \times 10^{-3} \text{ hr}^{-1}$ . At the high and low creep strain rate,  
 125 this corresponds to approximately a 7.4 and 2.2  $\mu\text{m}$  change in thickness over 23 hours,  
 126 respectively. Therefore, a wet membrane exhibits a higher creep resistance, after the first  
 127 hour, than the dry membrane. Additionally, the total creep decreases with increasing stress  
 128 when the membrane is wet. Thus, increasing hydration reduces the magnitude of creep  
 129 occurring in PFSA membranes under compression: the higher the pressure, the lower the thickness  
 130 change due to creep. This is an important outcome for PEM mechanical stability in high-  
 131 pressure electrolyzers as the membranes undergo higher stresses in hydrated conditions.

Table 1: Creep strain and displacement rates for the experiments on Nafion 117.

Hydration State	Applied Pressure [MPa]	Length of Experiment [hr]	Creep Strain Rate $\times 10^3$ [ $\mu\text{m}/\mu\text{m}/\text{hr}$ ]	Creep Displacement Rate [ $\mu\text{m}/\text{hr}$ ]
Dry	5	120	0.634	0.096
Dry	5	24	0.979	0.148
Dry	35	24	1.72	0.219
Wet	5	24	2.81	0.473
Wet	10	24	3.83	0.646
Wet	15	24	3.20	0.402
Wet	35	24	2.32	0.257

132 Figure 4a shows the effect of the applied compression load (pressure level) on the creep  
 133 response of hydrated Nafion membranes at 25 °C. With increasing stress, the initial and  
 134 total strain increase monotonically, as expected (Figure 4b). However, the creep strain de-  
 135 creases with increasing stress. This could be attributed to the hindered mobility of ionomer  
 136 aggregates and backbone chains under higher pressures in a phase-separated morphology  
 137 wherein less compressible water domains are trapped. When the hydrated ionomer is held  
 138 compressed, the ability of the polymer chains to accommodate the deformation by changing  
 139 their conformation is suppressed. It has been observed that membrane domain spacing be-  
 140 comes smaller in the direction of applied pressure and elongate in the plane of the membrane  
 141 to accommodate the nanostructural orientation effects.<sup>12</sup> In addition, resistance to nanoscale  
 142 deformation caused by the load-bearing hydrophobic domains is exacerbated further by the  
 143 additional restrictions imposed by the hydrophilic domains filled with incompressible water.

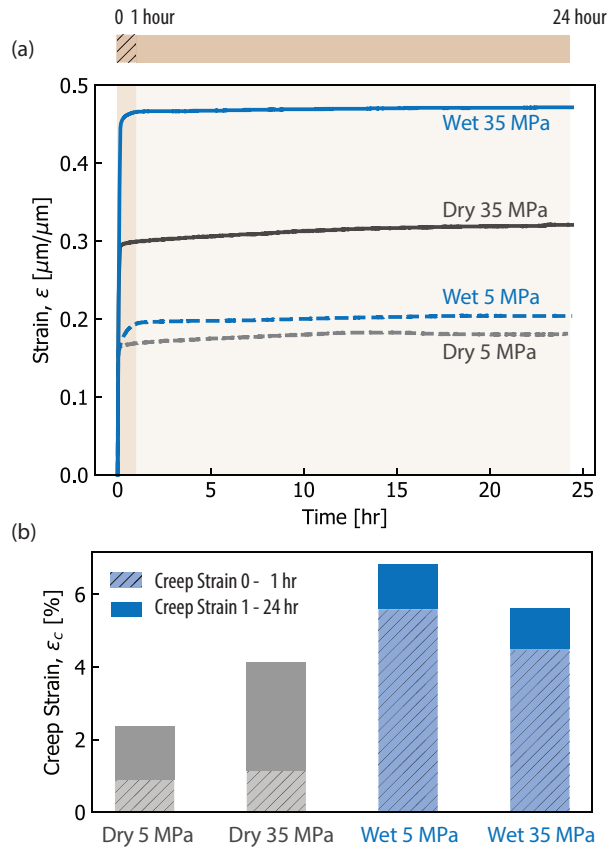


Figure 3: (a) Compression creep of pretreated Nafion 117 at 5 and 35 MPa and in dry and wet conditions. (b) Creep strain of these tests with the creep strain of the first hour in blue and the creep strain after the first hour in orange.

144 These hydrophilic domains act, mechanically, as occlusions, thereby increasing the creep  
 145 stiffness of the structure, and reducing creep strain.

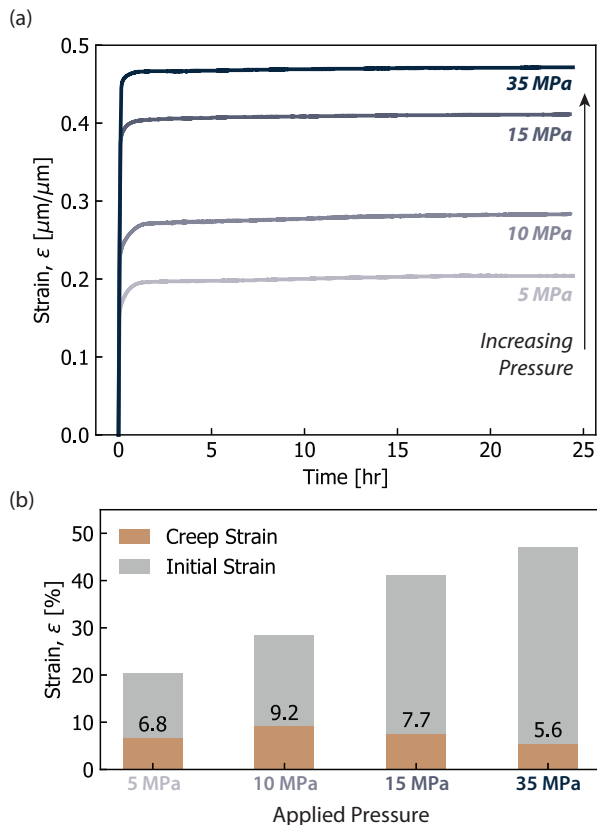


Figure 4: (a) Compression creep of wet preboiled Nafion 117 at 5, 10, 15, and 35 MPa of applied stress. The 5 MPa and 35 MPa curves are also shown in Figure 3. (b) The total strain decomposed into creep strain and initial strain as a function of applied stress. With increasing stress, the initial strain increases, but the creep strain decreases. The tan and gray color for creep and initial strain correspond to the colors used in Figure 2.

146 Membrane thickness is a key design parameter that directly contributes to the Ohmic  
 147 resistance in the cell. Thus, it is of interest to understand how reducing thickness for im-  
 148 proved ohmic losses would impact creep behavior. Table 2 shows the results from the creep  
 149 compression on three hydrated membranes with different thicknesses: Nafion 1110 (250  $\mu\text{m}$ ),  
 150 117 (175  $\mu\text{m}$ ), and 115 (125  $\mu\text{m}$ ). Thickness should not affect intrinsic response of a polymer  
 151 but it could affect the creep compliance because of geometric factors. In a hydrated state,  
 152 the thinnest membrane creeps the least with 5.58% creep strain over 24 hours.

153 The findings in this study demonstrate that mechanical response of PEM during mono-

Table 2: Creep strain, creep strain rates, and creep displacement rates for preboiled Nafion 1110, 117, and 115. The conditions of the experiments are wet, 35 MPa, at 25 °C, and held for 24 hours

Material Name	Nominal Thickness [ $\mu\text{m}$ ]	Creep Strain [%]	Creep Strain Rate $\times 10^3$ [ $(\mu\text{m}/\mu\text{m})/\text{hr}$ ]	Creep Displacement Rate [ $\mu\text{m}/\text{hr}$ ]
Nafion 1110	250	5.67	2.36	0.392
Nafion 117	175	5.60	2.32	0.257
Nafion 115	125	5.58	2.22	0.127

154 tonic loading changes dramatically from tension to compression, a mode that is not widely  
 155 studied despite its relevance to energy devices. Using a custom-designed *in situ* compression  
 156 setup, creep response of PEMs is demonstrated using PFSA membranes in both dry and  
 157 hydrated states. Creep is observed to occur over 24 hours and beyond (at least five days as  
 158 shown in Table 1) and exhibits dependence on hydration, membrane thickness, and applied  
 159 pressure levels. In hydrated state, Nafion membranes exhibit a creep strain rate of 0.2-0.3%  
 160 change in thickness per hour, depending on the pressure level. During creep compression,  
 161 a hydrated PFSA is more resistant to creep but exhibits a stronger dependence on stress  
 162 level. These findings translate into suppressed thickness reduction in the membrane under  
 163 high-compression regions, and possibly a non-uniform thickness change over time during cell  
 164 operation. Considering that membranes in electrolyzers must be optimized for thickness,  
 165 cost, performance, and mechanical stability over long times, these results show operating  
 166 parameters, such as pressure and hydration, could have significant impact on membrane  
 167 durability, with key implications also for membrane conductive resistance.

168 For example, Kaddouri et al.<sup>30</sup> have studied the effects of static compressive stress on an  
 169 extruded Nafion membrane’s water self-diffusion and have demonstrated a reduced diffusion  
 170 in the direction of applied compression (up to 10 MPa), particularly at higher humidities  
 171 ( $\geq 95\%$  RH). This anisotropy in diffusion is attributed to the structural changes within the  
 172 membrane, which is expected to increase further at higher pressures accessed in this study.  
 173 At higher pressures, the deformation may be irreversible and thus, a plastic deformation  
 174 of the membrane would exhibit a permanent reduction in water sorption. Kusoglu et al.<sup>12</sup>

175 have demonstrated that as the membrane is compressed, its water content decreased and  
176 its hydrophilic domain spacing inferred from SAXS studies decreases in the direction of  
177 the applied load, thereby affecting the proton conductivity within the membrane. The  
178 conductivity decreases with increasing pressure especially at higher humidities and in liquid  
179 water, in agreement with the nanostructural orientation observed under those conditions.

180 In summary, mechanical compression creates a unique environment for PEMs, espe-  
181 cially under high-compression loads and in hydrated state, as is the case in electrolyzer  
182 devices. On one hand, continuous creep reported in this work reduces the membrane thick-  
183 ness, thereby possibly altering the membrane-electrode interface and overall Ohmic resistance  
184 over time. On the other hand, based on prior studies denoting a strong morphological link  
185 between transport properties and morphological changes, such as intrinsic orientation and  
186 domain-alignment due to deformation, one would also anticipate changes in water content  
187 and transport properties under compression load. These affects altogether impact membrane  
188 performance and stability in an electrolyzer device. Hence, this study has shown that me-  
189 chanical stability for electrolyzer membranes could be characterized using compression loads  
190 and creep, which would have implications not only for longevity of PEMs, but also for their  
191 properties relevant to operation.

192 This work demonstrates that characterizing the mechanical response of polymer-electrolyte  
193 membranes under conditions relevant to device operation, such as compressive creep rate,  
194 is important and must be accounted for in material research for energy and environmental  
195 devices. Also, state-of-the-art PEMs are being challenged to operate at higher temperatures  
196 and stresses in an effort to further improve device efficiency and reduce operating costs to  
197 address the needs of emerging energy challenges. Therefore, future investigations could ex-  
198 plore the effects of various operating environments on the creep response and mechanical  
199 stability of electrolyte membranes, and factors related to cell assembly conditions and device  
200 design.

## 201 **Acknowledgement**

202 This work was carried out under HydroGEN and H2NEW consortia, funded by the Hydro-  
203 gen and Fuel Cell Technologies Office (HCTO), of the office of the Energy Efficiency and  
204 Renewable Energy (EERE), of the U.S. Department of Energy under contract number DE-  
205 AC02-05CH11231. The authors would like to thank Chris Capuano of Nel Hydrogen for very  
206 helpful research discussions. We thank Douglas Kushner for his help with the experimental  
207 setup, and Adam Weber and Nemanja Danilovic for their insightful perspectives.

## 208 **Supporting Information Available**

209 Associated Content: Full experimental methods are provided in detail in Supporting Infor-  
210 mation.

## 211 **References**

- 212 (1) Ayers, K. E.; Renner, J. N.; Danilovic, N.; Wang, J. X.; Zhang, Y.; Maric, R.; Yu, H.  
213 Pathways to ultra-low platinum group metal catalyst loading in proton exchange mem-  
214 brane electrolyzers. *Catalysis Today* **2016**, *262*, 121–132.
- 215 (2) Ayers, K. E.; Anderson, E. B.; Capuano, C.; Carter, B.; Dalton, L.; Hanlon, G.;  
216 Manco, J.; Niedzwiecki, M. Research Advances towards Low Cost, High Efficiency  
217 PEM Electrolysis. *ECS Transactions* **2010**, *33*, 3–15.
- 218 (3) Danilovic, N.; Ayers, K. E.; Capuano, C.; Renner, J. N.; Wiles, L.; Pertoso, M. (Ple-  
219 nary) Challenges in Going from Laboratory to Megawatt Scale PEM Electrolysis. *ECS*  
220 *Transactions* **2016**, *75*, 395–402.
- 221 (4) Carmo, M.; Fritz, D. L.; Mergel, J.; Stolten, D. A comprehensive review on PEM water  
222 electrolysis. *International Journal of Hydrogen Energy* **2013**, *38*, 4901–4934.

- 223 (5) Babic, U.; Suermann, M.; Büchi, F. N.; Gubler, L.; Schmidt, T. J. Critical Re-  
224 view—Identifying Critical Gaps for Polymer Electrolyte Water Electrolysis Develop-  
225 ment. *Journal of The Electrochemical Society* **2017**, *164*, F387–F399.
- 226 (6) Suermann, M.; Bensmann, B.; Hanke-Rauschenbach, R. Degradation of Proton Ex-  
227 change Membrane (PEM) Water Electrolysis Cells: Looking Beyond the Cell Voltage  
228 Increase. *Journal of The Electrochemical Society* **2019**, *166*, F645–F652.
- 229 (7) Department of Energy, *Department of Energy Hydrogen Program Plan*; 2020; pp 1–51.
- 230 (8) Cropley, C. C.; Norman, T. J. Low-Cost High-Pressure Hydrogen Generator. **2008**,  
231 N.p.
- 232 (9) Aricò, A. S.; Siracusano, S.; Briguglio, N.; Baglio, V.; Di Blasi, A.; Antonucci, V.  
233 Polymer electrolyte membrane water electrolysis: Status of technologies and potential  
234 applications in combination with renewable power sources. *Journal of Applied Electro-*  
235 *chemistry* **2013**, *43*, 107–118.
- 236 (10) Stucki, S.; Scherer, G. G.; Schlagowski, S.; Fischer, E. PEM water electrolyzers: Evi-  
237 dence for membrane failure in 100 kW demonstration plants. *Journal of Applied Elec-*  
238 *trochemistry* **1998**, *28*, 1041–1049.
- 239 (11) Kusoglu, A.; Weber, A. Z. New Insights into Perfluorinated Sulfonic-Acid Ionomers.  
240 *Chemical Reviews* **2017**, *117*, 987–1104.
- 241 (12) Kusoglu, A.; Hexemer, A.; Jiang, R.; Gittleman, C. S.; Weber, A. Z. Effect of com-  
242 pression on PFSA-ionomer morphology and predicted conductivity changes. *Journal of*  
243 *Membrane Science* **2012**, *421-422*, 283–291.
- 244 (13) Kusoglu, A.; Savagatrup, S.; Clark, K. T.; Weber, A. Z. Role of Mechanical Factors in  
245 Controlling the Structure–Function Relationship of PFSA Ionomers. *Macromolecules*  
246 **2012**, *45*, 7467–7476.

- 247 (14) Kusoglu, A.; Tang, Y. L.; Lugo, M.; Karlsson, A. M.; Santare, M. H.; Cleghorn, S.;  
248 Johnson, W. B. Constitutive response and mechanical properties of PFSA membranes  
249 in liquid water. *Journal of Power Sources* **2010**, *195*, 483–492.
- 250 (15) Satterfield, M. B.; Benziger, J. B. Viscoelastic properties of nafion at elevated temper-  
251 ature and humidity. *Journal of Polymer Science, Part B: Polymer Physics* **2009**, *47*,  
252 11–24.
- 253 (16) Tang, Y.; Karlsson, A. M.; Santare, M. H.; Gilbert, M.; Cleghorn, S.; Johnson, W. B.  
254 An experimental investigation of humidity and temperature effects on the mechanical  
255 properties of perfluorosulfonic acid membrane. *Materials Science and Engineering: A*  
256 **2006**, *425*, 297 – 304.
- 257 (17) Kawano, Y.; Wang, Y.; Palmer, R. A.; Aubuchon, S. R. Stress-Strain Curves of Nafion  
258 Membranes in Acid and Salt Forms. *Polímeros* **2002**, *12*, 96–101.
- 259 (18) Kusoglu, A.; Tang, Y.; Santare, M. H.; Karlsson, A. M.; Cleghorn, S.; Johnson, W. B.  
260 Stress-strain behavior of perfluorosulfonic acid membranes at various temperatures and  
261 humidities: Experiments and phenomenological modeling. *Journal of Fuel Cell Science*  
262 *and Technology* **2009**, *6*, 0110121–0110128.
- 263 (19) Silberstein, M. N.; Boyce, M. C. Constitutive modeling of the rate, temperature, and  
264 hydration dependent deformation response of Nafion to monotonic and cyclic loading.  
265 *Journal of Power Sources* **2010**, *195*, 5692 – 5706.
- 266 (20) Tang, Y.; Kusoglu, A.; Karlsson, A. M.; Santare, M. H.; Cleghorn, S.; Johnson, W. B.  
267 Mechanical properties of a reinforced composite polymer electrolyte membrane and its  
268 simulated performance in PEM fuel cells. *Journal of Power Sources* **2008**, *175*, 817–825.
- 269 (21) Elliott, J.; Hanna, S.; Newton, J.; Elliott, A.; Cooley, G. Elimination of Orientation in  
270 Perfluorinated Ionomer Membranes. *Polym Eng Sci* **2006**, *46*, 228–234.



- 271 (22) Li, J.; Wilmsmeyer, K. G.; Madsen, L. A. Anisotropic diffusion and morphology in  
272 perfluorosulfonate ionomers investigated by NMR. *Macromolecules* **2009**, *42*, 255–262.
- 273 (23) Park, J. K.; Li, J.; Divoux, G. M.; Madsen, L. A.; Moore, R. B. Oriented morphol-  
274 ogy and anisotropic transport in uniaxially stretched perfluorosulfonate ionomer mem-  
275 branes. *Macromolecules* **2011**, *44*, 5701–5710.
- 276 (24) Mendil-Jakani, H.; Pouget, S.; Gebel, G.; Pintauro, P. N. Insight into the multiscale  
277 structure of pre-stretched recast Nafion® membranes: Focus on the crystallinity fea-  
278 tures. *Polymer* **2015**, *63*, 99–107.
- 279 (25) Budinski, M. K.; Cook, A. Osmotic Pressure of Water in Nafion®. *Tsinghua Science*  
280 *and Technology* **2010**, *15*, 385–390.
- 281 (26) Kusoglu, A.; Kienitz, B. L.; Weber, A. Z. Understanding the Effects of Compression and  
282 Constraints on Water Uptake of Fuel-Cell Membranes. *Journal of The Electrochemical*  
283 *Society* **2011**, *158*, B1504.
- 284 (27) Majsztrik, P. W.; Bocarsly, A. B.; Benziger, J. B. Viscoelastic response of nafion. effects  
285 of temperature and hydration on tensile creep. *Macromolecules* **2008**, *41*, 9849–9862.
- 286 (28) Zhang, Z.; Tian, C.; Yuan, Z.; Li, J.; Wu, W. P.; Xia, R. Temperature and load-  
287 ing sensitivity investigation of nanoindentation short-term creep behavior in Nafion®.  
288 *Materials Research Express* **2019**, *6*, 055304.
- 289 (29) Satterfield, M. B.; Majsztrik, P. W.; Ota, H.; Benziger, J. B.; Bocarsly, A. B. Mechanical  
290 Properties of Nafion and Titania/Nafion Composite Membranes for Polymer Electrolyte  
291 Membrane Fuel Cells. *Journal of Polymer Science: Part B: Polymer Physics* **2006**, *44*,  
292 2327–2345.
- 293 (30) El Kaddouri, A.; Perrin, J.-C.; Colinart, T.; Moyne, C.; Leclerc, S.; Guendouz, L.;  
294 Lottin, O. Impact of a Compressive Stress on Water Sorption and Diffusion in Ionomer

295 Membranes for Fuel Cells. A  $^1\text{H}$  NMR Study in Vapor-Equilibrated Nafion. *Macro-*  
296 *molecules* **2016**, *49*, 7296–7307.

297 **Graphical TOC Entry**

298

